European Journal of Neuroscience, Vol. 24, pp. 1001–1010, 2006 doi:10.1111/j.1460-9568.2006.05000.x

Transient synaptic zinc-positive thalamocortical terminals in the developing barrel cortex

Noritaka Ichinohe,[1,2] Daniel Potapov[1] and Kathleen S. Rockland[1,3]
[1]Laboratory for Cortical Organization and Systematics, Brain Science Institute, RIKEN, 2-1 Hirosawa, Wako-shi, Saitama 351-0198, Japan
[2]Graduate School of Medicine, Kyoto University, Japan
[3]Graduate School of Science and Engineering, Saitama University, Japan

Keywords: brain-derived neurotrophic factor, glutamatergic system, plasticity, rat, synaptogenesis

Abstract

In rat barrel cortex, layer 4 has a transiently high density of zinc-positive terminations from postnatal day (P)9 to P12 [P.W. Land & L. Shamalla-Hannah (2002) *J. Comp. Neurol.*, **447**, 43–56]. These terminations have been proposed to originate from cortico-cortical connections, but their exact origin is unknown. To determine their sources, we injected sodium selenite into the barrel cortex of two adult rats and 32 pups, from P5 to P28. As predicted, abundant zinc-positive cortically projecting neurons were visible around the injection sites and in distant cortical areas. From P9 to P13, however, neurons retrogradely labeled by zinc selenite occurred in the thalamus, in topographically appropriate regions of the ventroposterior medial (VPM) and posterior nuclei (Po). Because there are no previous reports of zinc-positive sensory thalamocortical connections, we sought corroboration of this unexpected finding by electron microscopy. This revealed a subset of boutons in layers 4 and 1, positive for both zinc and vesicular glutamate transporter 2, a protein used by thalamocortical terminations. Finally, in an additional nine rats, we carried out *in situ* hybridization for zinc transporter 3 mRNA. Moderate signal was detected in VPM and Po at P10, but this disappeared by P28. In contrast, a strong signal was apparent in the anterodorsal nucleus, which projects to limbic areas, and this persisted at P28. The timing of the transient zinc-positive terminations in the sensory thalamus roughly coincides with the onset of exploratory and whisking behavior in the middle of the second postnatal week; and this suggests zinc is important for activity-related refinement of circuitry.

Introduction

Synaptic or vesicular zinc is associated with a subset of non-thalamic glutamatergic terminations, and has been implicated in both experience-related and developmentally related plasticity (Brown & Dyck, 2002; Land & Shamalla-Hannah, 2002; Czupryn & Skangiel-Kramska, 2003; Dyck *et al*., 2003; see for review Frederickson *et al*., 2005). In the barrel cortex, layer 4 is zinc-poor in the adult, but has a transient high density of zinc-positive terminations from postnatal day 9 (P9) to P12 (Land & Shamalla-Hannah, 2002). This postdates the critical period for barrel cytoarchitectural formation (P0–P7: see for review Fox, 2002; Lopez-Bendito & Molnar, 2003). It roughly coincides with the onset of normal whisking behavior (at about P12: Welker, 1964) and the refinement of thalamocortical and corticocortical connections (Agmon *et al*., 1993; Portera-Cailliau *et al*., 2005). This includes a heightened rate of synaptogenesis (P10–P15; Micheva & Beaulieu, 1996; P8–P12, De Felipe *et al*., 1997) and a high degree of turnover and motility of dendritic spines (Lendvai *et al*., 2000).

The period of transient zinc-positive terminations thus coincides with multiple developmental processes occurring during the second postnatal week. In investigating the potential influence of the transient zinc, one question pertains to the origin of these terminations. A reasonable hypothesis is that they originate from neurons in layers 2 and/or 3 of the barrel cortex itself, as synaptic zinc is preferentially used by corticocortical connections in the adult (Garrett *et al*., 1992; Casanovas-Aguilar *et al*., 1995, 1998, 2002; Brown & Dyck, 2004). These cortical terminations may be subsequently pruned or may have a transient, stage-specific ability to sequester and utilize zinc (Land & Shamalla-Hannah, 2002). A thalamic origin has seemed less likely, given the absence of zinc in thalamocortical terminations in the adult (Garrett *et al*., 1992; Casanovas-Aguilar *et al*., 1998; Brown & Dyck, 2004).

In the rat granular retrosplenial cortex (GRS), there is also a similar transient increase of zinc-positive terminations, in three strata of layer 1, most pronounced at P13–P15 (Miro-Bernie *et al*., 2006). Based on three corroborating pieces of evidence, we suggested that the transient zinc-positive terminations in one system originated from neurons in the anterodorsal (AD) thalamus. Most dramatically, inspection by electron microscopy (EM) confirmed the localization of zinc in synaptic boutons labeled by vesicular glutamate transporter 2 (VGluT2), a protein typically used by thalamocortical terminations (Fujiyama *et al*., 2001); and intracortical injection of the tracer sodium selenite at P9 and P13 resulted in retrogradely labeled zinc-positive neurons in the AD thalamic nucleus.

These findings in the GRS raised the question of whether the transient zinc-positive terminations in the barrel cortex might also have a thalamocortical source; and we accordingly carried out appropriate experiments in the barrel cortex of young rats. In fact, sodium selenite injections at P9–P13 produced zinc-positive neurons in the primary somatosensory thalamus, and EM inspection revealed boutons positive for both zinc and VGluT2. Further, *in situ* hybridization for zinc transporter 3 (ZnT3) mRNA revealed labeled

Correspondence: Dr N. Ichinohe, as above.[1]
E-mail: nichinohe@brain.riken.jp

Received 13 February 2006, revised 11 June 2006, accepted 14 June 2006

neurons in the ventroposterior medial (VPM) and posterior (Po) nuclei at P10, but not at P28.

Materials and methods

Animals and tissue preparation

A total of 32 rat pups of both sexes (P5, 3; P7, 5; P9, 2; P10, 3; P13, 3; P15, 4; P18, 4; P21, 4; P22, 2; P28, 2) and two adult male Wistar rats were used to investigate the origin of zinc-positive terminals in the barrel field (see 'Retrograde tracing'). An additional two pups at P10 and two adults were used for the EM study. Nine pups (three each at P3, P10 and P28) were used for *in situ* hybridization for ZnT3 mRNA. All experimental procedures described here were approved by the Experimental Animal Committee of the RIKEN Institute, and were carried out in accordance with institutional guidelines. In this study, the day of birth is designated P0.

Retrograde tracing

Rats were anesthetized with Nembutal intraperitoneally (100 mg/kg), placed in a stereotaxic frame, and administered pressure injections of 0.2 μL of 0.1% sodium selenite (Sigma, St. Louis, MO, USA). For adults, the coordinates of Paxinos & Watson (1998) were used to locate the barrel cortex; that is, bregma −0.8 mm anteroposterior and 5.0 lateral (needle tilted 20–30 ° medial-wards). In younger animals, the coordinates for the injection site in the barrel cortex were determined empirically, as no stereotaxic atlas was available for these young animals. The midline suture and bregma were used as reference landmarks for determining the coordinates, and the distance between bregma and lambda was further taken into account. Additional animals, not counted in the total number 32, were used as trials. Animals were recovered and allowed to survive for 24 h, so that the zinc precipitated in synaptic boutons by the selenium injection was retrogradely transported back to cell somata (Christensen *et al*., 1992; Casanovas-Aguilar *et al*., 1995, 1998, 2002; Brown & Dyck, 2005). Animals were then re-anesthetized and perfused, first with 0.9% NaCl and 0.5% $NaNO_2$ for 1 min, and then 4% paraformaldehyde in 0.1 M phosphate buffer (pH 7.3, PB) for 5 min. Brains were removed and postfixed in 4% paraformaldehyde in 0.1 M PB for 2 h, and immersed into 30% sucrose in 0.1 M PB until sinking (20–40 h). Sections were cut (in the coronal plane, at 40 μm thickness) by a sliding microtome in two repeating series for older pups (> P9) or three repeating series for younger pups (P5, P7). For one series, sections were washed thoroughly with 0.1 M PB, followed by 0.01 M PB. The IntenSE M silver Enhancement kit (Amersham International; Little Chalfont, Bucks, UK) was used to intensify zinc signals (Danscher *et al*., 1987; De Biasi & Bendotti, 1988). A one-to-one cocktail of the IntenSE M kit solution and 33% gum arabic solution was used as a reagent. Development of reaction products was monitored under a microscope and terminated by rinsing the sections in 0.01 M PB and, subsequently, several rinses in 0.1 M PB. Selected sections were further processed for Nissl substrate using NeuroTrace 500/525 green fluorescent Nissl stain (Molecular Probes, Eugene, OR, USA) according to the company's protocol. Adjacent sections (in the second and/or third series) were stained for Nissl and/or for VGluT2 (a thalamocortical terminal marker, Fujiyama *et al*., 2001) immunohistochemistry to order to determine the location of the injection site and its relation to the barrel field. Sections were observed in brightfield or darkfield light microscopy.

The specificity of sodium selenite as a retrograde tracer for zinc has been discussed in Frederickson *et al*. (2000) and Brown & Dyck (2005). Recently, Land & Aizenman (2005) have reported that thalamic neurons degenerating subsequent to a large cortical lesion show zinc-selenite precipitate in their cell body after an intraperitoneal injection of sodium selenite. This zinc is liberated from intracellular stores (Aizenman *et al*., 2000), and visualized by complexing with sodium selenite. In our experiments, even if thalamic neurons had non-vesicular zinc in their somata owing to developmental apoptosis or injection damage, this zinc would be washed out during the perfusion, as there would be no source of selenite ions for crystallization except from the injection site. Thus, we can interpret our neurons as labeled by retrograde transport of zinc selenite crystals formed in the terminals at the injection site.

As further confirmation that zinc-selenite labeling is not attributable to a degeneration process, we carried out double-labeling ($n = 2$ pups at P10) for silver enhancement and Fluoro-Jade B, a standard fluorescent marker for degenerating neurons (Schmued *et al*., 1997; Riba-Bosch & Perez-Clausell, 2004). A sodium selenite injection was made as described above. After silver enhancement, sections were transferred to the staining solution containing 0.01% acetic acid and 0.0004% of the fluorochrome Fluoro-Jade B (Histo-Chem, Jefferson, AR, USA) for 20 min. A few Fluoro-Jade-positive neurons were found in the cortex, but these were restricted to within the central core of the injection site. No neurons were detected at a distance or in the thalamus.

Immunoperoxidase staining for VGluT2

Sections were incubated for 1 h with 0.1 M phosphate-buffered saline (PBS, pH 7.3) containing 0.5% Triton X-100 and 5% normal goat serum (PBS-TG) at room temperature, and then for 40–48 h at 4 °C with PBS-TG containing anti-VGluT2 polyclonal rabbit antibody (Synaptic Systems, Gottingen, Germany, 1 : 10 000). After rinsing, the sections were placed in PBS-TG containing biotinylated anti-rabbit IgG polyclonal goat antibody (Vector, Burlingame, CA, USA; 1 : 200) for 1.5 h at room temperature. Immunoreactivity was visualized by ABC incubation (one drop of reagents per 7 mL 0.1 M PB, ABC Elite kits; Vector) followed by diaminobenzidine histochemistry with 0.03% nickel ammonium sulfate.

EM analysis of boutons containing zinc and VGluT2 in the developing barrel hollow and layer 1

Two P10 pups and two adult rats were injected with 200 mg/kg sodium sulfide into the vena cava under conditions of deep anesthesia (Nembutal, 100 mg/kg). Two minutes after the injection, animals were perfused transcardially, in sequence, with 0.9% NaCl and 0.5% $NaNO_2$ for 1 min, 4% paraformaldehyde with 0.1% glutaraldehyde in 0.1 M PB for 5 min, and postfixed with the same fixative for 2 h. Vibratome-cut coronal sections (50 μm thick) were prepared. These were washed thoroughly with 0.1 M PB, followed by distilled water. The silver enhancement kit was used to intensify zinc signals as described above. Staining intensity during development was carefully monitored by periodic visual inspection under a low-power microscope. Development was terminated by rinsing the sections in distilled water and, subsequently, several times in 0.1 M PB. Several sections that included the barrel cortex were further processed for peroxidase-immunohistochemistry for VGluT2 as a means of identifying thalamocortical terminals (Fujiyama *et al*., 2001). The procedures for VGluT2 visualization were basically as described above for light microscopy, except that Triton X-100 was omitted in all solutions, and nickel was omitted for the diaminobenzidine step. To improve antibody penetration in the absence of Triton X-100, after silver enhancement, sections were incubated in 20% sucrose for 2 h, and then were freeze-thawed with liquid nitrogen.

Sections stained either for zinc alone, or for zinc and VGluT2, were osmicated, dehydrated (including treatment with 1% uranyl acetate in 70% ethanol) and flat-embedded in resin (Araldite M; TAAB, Aldermaston, UK). From the plastic sections, we further trimmed out layer 1 and the barrel hollow, which was easily identified as a zinc-weak portion in layer 4. Sampled barrels were from coronal sections at the level comparable to Bregma −1.4 mm. They were large in size and lateral to the medial-most barrels, in what may correspond to row C, D or E. Ultrathin sections were collected on formvar-coated, single-slot grids, and examined with an EM (JEM 2000-EX; JEOL, Tokyo, Japan). For quantification, EMs were taken at a magnification of 30 000 from randomly selected fields that included VGluT2-immunoreactive (ir) and zinc-positive elements in the neuropil. Data were collected from one tissue sample from each of the two pups and two adult animals. Data from the pups and adults were accumulated separately. A total of 50 micrographs, equivalent to 1620 μm^2 of tissue, were scanned for both pups and adults. Digital pictures were recorded. Brightness and contrast of these were adjusted, using imaging processing software, to correspond to the original images.

When critical steps are controlled (i.e. low sulfide concentrations and fixed amplification parameters) as in Danscher's procedure (Danscher, 1981, 1982), the sulfide method is reported to reveal zinc specifically associated to synaptic vesicles. That the signal is zinc, as opposed to other metal ions, is supported by several previous results. (1) Zinc distribution shown by silver amplification is coincident with that shown by specific zinc fluoroprobes (TSQ, zincquin: Frederickson *et al*., 1992; Woodroofe *et al*., 2004). (2) Previous treatment with zinc fluoroprobes or other metal chelators blocks the sulfide precipitation and the subsequent silver amplification. (3) Our EM data (see Results) clearly show that the silver reaction product is localized to synapses. Iron is reported to be localized mainly to the nucleus of neurons and glia (Yu *et al*., 2001), and copper mainly to glia (Szerdahelyi & Kasa, 1986).

In previous experiments (Miro-Bernie *et al*., 2006), we injected two rats at P10 with the chelating agent diethyldithiocarbamate (500 mg/kg, intraperitoneally) and, 1 h later, the animals were perfused with sulfide as described here. No subsequent staining was observed in the neocortex, supporting the specificity of the staining. Given these controls, we accept that the observed staining is specific for zinc and accordingly refer here to 'staining for zinc'.

In situ *hybridization for ZnT3*

PCR primers for ZnT3 (CTTCTCTATCTGCGCCCTTG and GAGCAGACTCACAACGACCA) were designed based on the rat cDNA sequence of ZnT3 (GenBank No. NM001013243). The DNA fragments were produced by reverse transcriptase-polymerase chain reaction (RT-PCR) from rat cDNA. PCR fragments were ligated into the pBluescript II (KS +) vector. The plasmids were extracted and linearized by *Asp718* or *Xho1* before being used for the template of antisense or sense probes. The digoxigenin (DIG)-dUTP labeling kit (Roche, Basel, Switzerland) was used for *in vitro* transcription.

Nine pups (three each at P3, P10 and P28) were used for *in situ* hybridization for ZnT3 mRNA. Pups were anesthetized with Nembutal intraperitoneally (100 mg/kg), and perfused transcardially, in sequence, with distilled water containing 0.9% NaCl and 0.5% $NaNO_2$ for 1 min, and 4% paraformaldehyde in 0.1 M PB for 10 min. Brains were removed and postfixed in the same fixative for 2 h, and then immersed into 30% sucrose in 0.1 M PB until sinking (20–40 h). Sections were cut (in the coronal plane, at 30 μm thickness) by using a sliding microtome, mounted on glass slides and dried. Sections on slides were washed in 0.1 M PB, and again postfixed with 4% paraformaldehyde in 0.1 M PB for 10 min. After washing in 0.1 M PB, sections were treated with 1 μg/mL proteinase K for 10 min at 37 °C, acetylated, then incubated in hybridization buffer containing 0.5–1.0 μg/mL DIG-labeled riboprobes at 60 °C. The sections were sequentially treated for 15 min at 55 °C in 2 × standard sodium citrate (SSC)/50% formamide/0.1% N-lauroylsarcosine, twice; for 30 min at 37 °C in RNase buffer (10 mM Tris–HCl, pH 8.0, 1 mM EDTA, 500 mM NaCl) containing 20 μg/mL RNase A (Sigma, St. Louis, MO, USA); for 15 min at 37 °C in 2 × SSC/0.1% N-lauroylsarcosine, twice; for 15 min at 37 °C in 0.2 × SSC/0.1% N-lauroylsarcosine, twice. The hybridized probe was detected by alkaline phosphatase-conjugated anti-DIG antibody with DIG detection kits (Roche Diagonostics, Basel, Switzerland). Control of hybridization with sense strand-labeled riboprobes showed no hybridization signal (Fig. 5C and F).

Data analysis

Areal, laminar and nuclear boundaries were defined by: (1) direct fluorescent Nissl counterstain in the same sections reacted for zinc; and (2) comparison between zinc-reacted sections and adjacent sections stained for Cresyl violet or VGluT2. The nomenclature and abbreviations for cortical areas and thalamic nuclei follow Paxinos & Watson (1998).

Results

Definition of the injection site

As shown in Fig. 1, the selenium injection site could be easily verified by the presence of zinc histochemical reaction product surrounding the needle track. Three zones were distinguished: (1) a central core with black or dark brown uniform color; (2) a transition area where the black color was less intense and cell bodies could be distinguished; and (3) a pale halo, seen only in darkfield illumination, which could correspond to dense local anterograde transport and/or tracer diffusion. According to previous studies (Casanovas-Aguilar *et al*.,

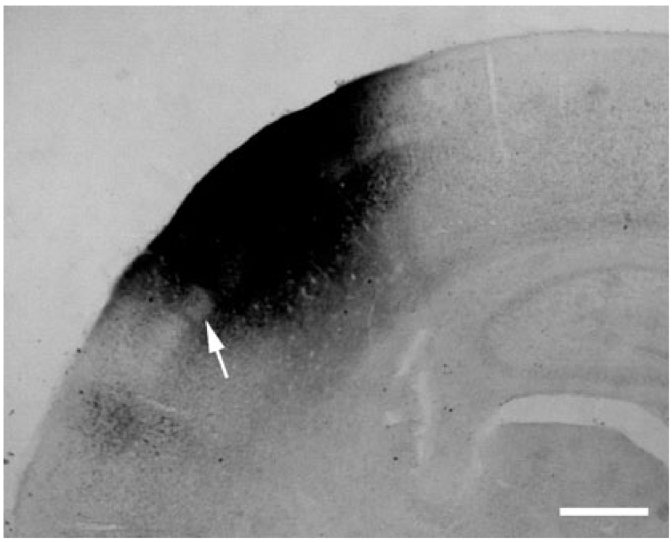

FIG. 1. Photomicrograph of a sodium selenite injection in the developing barrel cortex of a P9 pup. Coronal view, where medial is to the right. The barrel hollow can be recognized as the lightly stained area (Arrow). Scale bar, 500 μm.

1998, 2002), the uptake and retrograde transport of metal precipitates can be associated with the core of the injection.

The injections were measured as 0.5–1.0 mm medio-lateral, and typically encompassed all cortical layers. In some cases the injection invaded the medially adjacent dysgranular cortex (Killackey, 1983) or penetrated shallowly (0.2 mm) into the underlying striatum. For these larger injections, comparisons were available at all stages with more restricted injections. From P9, localization of the injection within the barrel field could be ascertained by the appearance of zinc-weak hollows and zinc-enriched septa within the fringe of the injection (Fig. 1). We estimate that at least three–four barrels (probably from medially situated rows C–E) are included in our injections. Zinc-positive cortical neurons were conspicuous both in distant areas and around the injection sites, as will be described in detail elsewhere (Ichinohe *et al*., 2006).

Retrograde labeling of zinc-positive neurons in the thalamus

Injections within the barrel cortex at P5 ($n = 3$) or P7 ($n = 5$) do not result in any detectable thalamic labeling. In contrast, injections at P9 ($n = 2$) and P10 ($n = 3$) produce zinc-positive neurons in both the VPM and Po (Figs 2 and 3). At P13, two of three cases had labeled neurons; but from P15 ($n = 4$), injections do not reveal any labeled neurons in either VPM or Po.

The labeled thalamic neurons occurred in both VPM and Po (Figs 2 and 3). In VPM, labeled cells formed one continuous projection focus with an oblique orientation from the anterodorso-medial to the posteroventro-lateral direction. Labeled cells occurred preferentially in the anterior half of VPM, in a dorsolateral location. These features are appropriate to the intended location of our injection sites, as judged by reference to electrophysiological data, concerning the whisker field map, especially of the ventral row, C–E (Waite, 1973; Sugitani *et al*., 1990), and anatomical data, concerning thalamocortical connections for row C–E (Land & Simons, 1985; Land *et al*., 1995). The projection focus tended to be largest in the anterior plane (diameter = 200–500 μm), with a total anterior-posterior extent of 300–800 μm. Because the diameter of one barreloid is 100–150 μm (Land *et al*., 1995), we infer that our injection involved several barrels.

The labeled cells in the Po tended to occur laterally and dorsally in the region having anatomical connections with the whisker barrel cortex (Fabri & Burton, 1991; Diamond *et al*., 1992). Comparing the number of labeled neurons in the densest area with the total number of cells, seen in fluorescent Nissl staining, we estimate about half of VPM cells and one-third of Po cells are zinc-positive.

In the cases where the injection involved the dorsal striatum, zinc-positive neurons are evident in the parafascicular nucleus, centrolateral nucleus and laterodorsal nucleus (data not shown). These occurred transiently from P5 to P13.

EM

Previous light microscopic studies (Land & Shamalla-Hannah, 2002) have reported that zinc-positive terminations are elevated in the barrel hollow from P9 to P12, in contrast with the adult distribution, where the barrel hollows are zinc-poor. Consistent with this result, EM analysis at P10 of the neuropil within the barrel hollow easily demonstrated zinc-positive synapses (Fig. 4A). In addition, in P10 pups, double-labeling procedures revealed a subset of presynaptic boutons positive for both VGluT2 and zinc. Of 200 VGluT2-ir terminals, 21 (or 10%) were zinc-positive (Fig. 4B and C). Postsynaptic targets of the double-labeled terminals consisted of both thin dendrites and dendritic spines, but were mainly spines ($n = 18$ of 21 postsynaptic profiles, or 85%). In adults, in contrast, none of the VGluT2-ir terminals ($n = 340$) was identified as zinc-positive (Fig. 4D). This is in agreement with the absence of retrogradely labeled neurons in the adult thalamus after sodium selenite injections into the barrel cortex. Furthermore, of 57 zinc-positive presynaptic terminals in P10 pups, 21 (or 37%) were VGluT2-ir and 36 (or 63%) were VGluT2-negative. In the adult, all inspected zinc-positive presynaptic terminals ($n = 12$) were VGluT2-negative, and are likely to be cortical in origin.

In addition, we examined layer 1, which receives dense projections from the Po (Herkenham, 1980; Lu & Lin, 1993). Results are similar to those for the barrel hollow in layer 4. In P10 pups, double-labeling procedures again revealed a subset of presynaptic boutons positive for both VGluT2 and zinc. Of 200 VGluT2-ir terminals, 31 (or 15%) were zinc-positive (Fig. 4E and F). Postsynaptic targets of double-labeled terminals consisted of both thin dendrites and dendritic spines, but were mainly spines ($n = 27$ of 31 postsynaptic profiles, or 87%). In adults, however, none of the VGluT2-ir terminals ($n = 340$) was identified as zinc-positive (not shown). This is in agreement with the absence of retrogradely labeled neurons in the adult thalamus after sodium selenite injection into the barrel cortex. Furthermore, of 130 zinc-positive presynaptic terminals in P10 pups, 60 (or 47%) were VGluT2-ir and 70 (or 53%) were VGluT2-negative. In the adult, all inspected zinc-positive presynaptic terminals ($n = 45$) were VGluT2-negative, and likely to be cortical in origin.

Expression pattern of ZnT3 mRNA in the developing thalamus

Several zinc transporter families have been identified, but their expression, trafficking and relation to free zinc is complex and under active investigation (e.g. Colvin *et al*., 2003). We concentrated on ZnT3, first reported by Palmiter *et al*. (1996), as most work in the brain has so far concentrated on this protein (see for review, Colvin *et al*., 2003).

As Valente & Auladell (2002) have reported, in P3 pup thalamus, ZnT3 mRNA was only very weakly and diffusely expressed (data are not shown). At P10, ZnT3 mRNA could be detected in every nucleus; but the level of expression differed from nucleus to nucleus (Fig. 5A and B). Most nuclei, including VPM and Po, where zinc-positive neurons were found in this study, contained neurons with weak-to-medium levels of ZnT3 expression. We observed that neurons strongly expressing ZnT3 mRNA were found in the paratenial, mediodorsal, centrolateral, ventral lateral geniculate and lateral habenular nuclei. Signal was observed in the dorsal lateral geniculate nucleus (LGN: visual thalamus) and medial geniculate body (MGB: auditory thalamus) but, as in the VPM and Po, this was only moderate. In addition, markedly strong ZnT3-labeling was obvious in the AD (where strong zinc-positive labeling occurred after sodium selenite injection in the GRS at P10, see Fig. 7 in Miro-Bernie *et al*. (2006). At P28, most thalamic nuclei no longer contained ZnT3 mRNA-expressing neurons, except for the paratenial, mediodorsal and lateral habenular nuclei (Fig. 5D and E). The signal remained strong in the AD, which is the single thalamic nucleus where zinc-positive projection neurons have been reported in the adult (Long & Frederickson, 1994).

Discussion

In adult rats, the thalamocortical synapses do not contain zinc, except for thalamocortical connections from the AD to the subiculum, which are zinc-positive (Garrett *et al*., 1992; Long & Frederickson, 1994; Casanovas-Aguilar *et al*., 1998; Brown & Dyck, 2004, 2005). Here, we nevertheless report that some sensory thalamocortical synapses from both VPM and Po are zinc-positive during the second postnatal

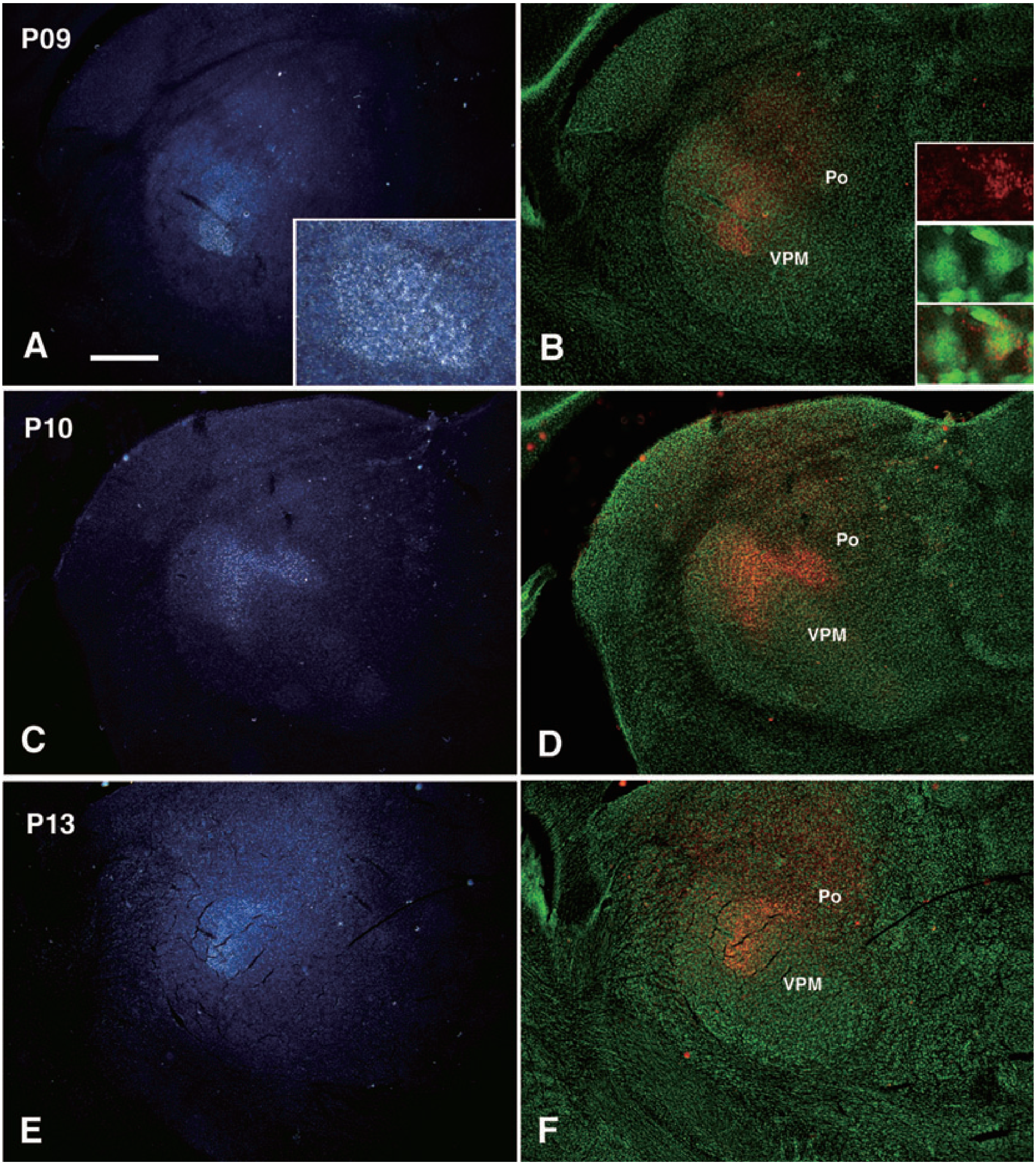

FIG. 2. Retrograde labeling of zinc-positive neurons in the developing thalamus at P9, P10 and P13. Left column: darkfield images of neurons retrogradely labeled by sodium selenite injections in the cortex. Cells are seen in both the ventroposterior medial nucleus (VPM) and posterior nucleus (Po). Inset in (A) is the enlarged image from VPM. Right column: same sections, where images of fluorescent Nissl have been merged with pseudo-colored darkfield images, to show the position of labeled neurons within the thalamic nuclei. Insets in (B) are enlarged images from VPM. Top: pseudo-colored darkfield image of a zinc-positive neuron; middle: fluorescent Nissl of the same neuron with adjacent non-labeled neurons; bottom: merged image. Scale bar, 150 μm for inset in (A); 20 μm for insets in (B); rest, 500 μm.

week, from P9 to P13. This is based on: (1) retrograde transport of zinc selenite crystals from a cortical injection to neurons in topographically appropriate regions of VPM and Po; (2) EM verification that some terminations positive for VGluT2 contain zinc; and (3) transient expression of ZnT3 mRNA in neurons in VPM and Po. The role of zinc transporters is complex (e.g. Colvin *et al*., 2003); and there have even been two reports in mouse of a temporal dissociation of synaptic zinc and ZnT3 expression during postnatal

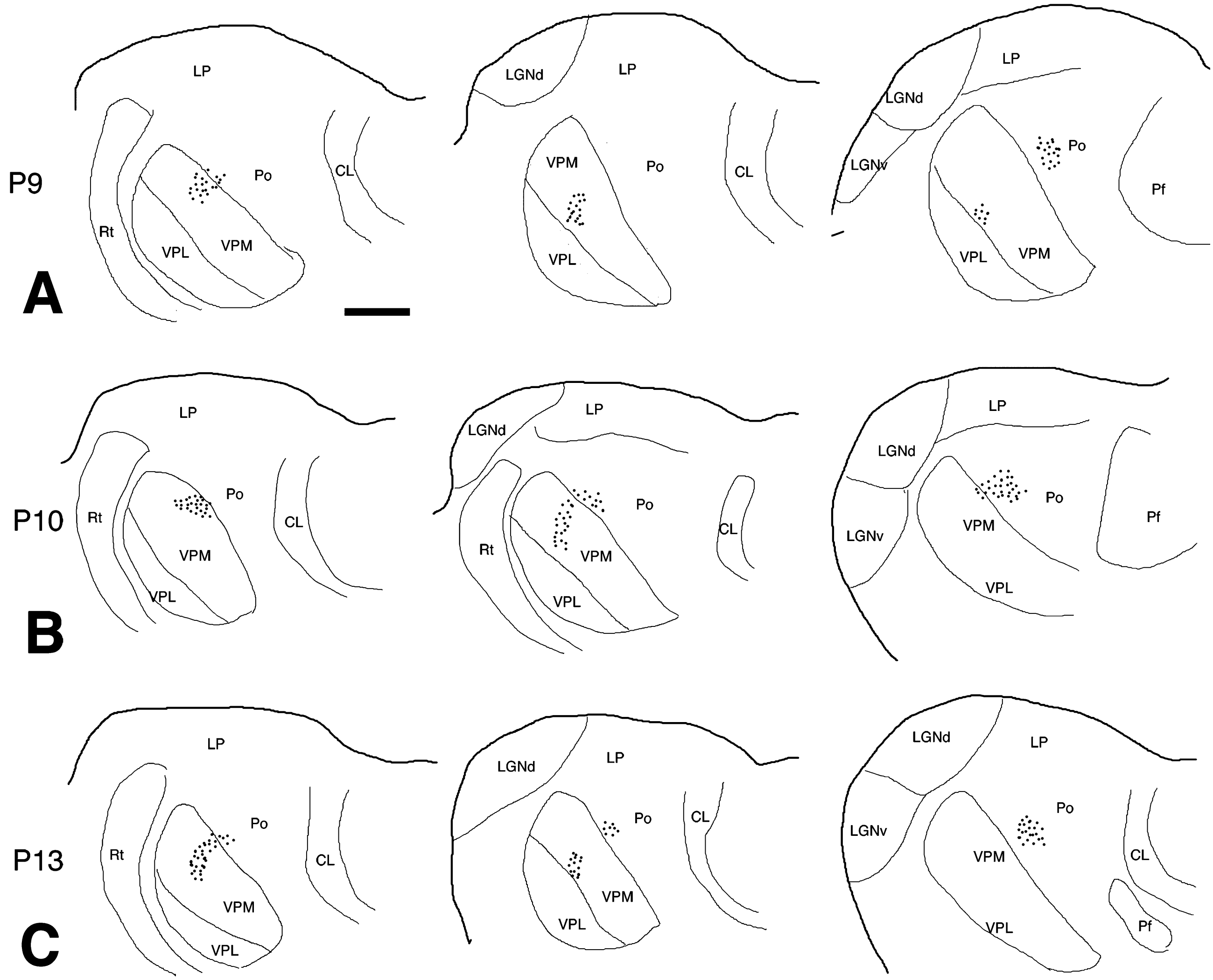

FIG. 3. Plots from coronal sections through the thalamus of three representative cases (A is from P9, B from P10, C from P13). Dots show the distribution of zinc-positive neurons, where one dot equals about five neurons. Spacing between sections is 200 μm. Scale bar, 500 μm. CL, central lateral nucleus; LGNd, lateral geniculate nucleus, dorsal part; LGNv, lateral geniculate nucleus, ventral part; LP, lateral posterior nucleus; Pf, parafascicular nucleus; Po, posterior nucleus; Rt, reticular nucleus of thalamus; VPL, ventroposterior lateral nucleus; VPM, ventroposterior medial nucleus.

development. That is, there is a delayed expression of ZnT3, until P14, in the barrel hollow (Valente & Auladell, 2002; Liguz-Lecznar *et al.*, 2005). In the present study, the three methods together present strong evidence for the occurrence of transient zinc-positive neurons in VPM and Po. *In situ* hybridization also showed neurons expressing ZnT3 mRNA in other thalamic nuclei, including the LGN and MGB. In the sensory thalamic nuclei, however, expression is only moderate and is transient in nature. This contrasts with neurons in AD, where ZnT3 mRNA is expressed strongly and persistently. [AD gives rise to a transient zinc-positive thalamocortical projection to the GRS (Miro-Bernie *et al.*, 2006), but persistent zinc-positive projections to the subiculum.] Further investigations are needed to address these differences between limbic and sensory thalamocortical systems.

Transient expression of synaptic zinc has been reported in the retinogeniculate pathway, specifically in the uncrossed pathway (Land & Shamalla-Hannah, 2001). The duration of zinc staining in the LGN overlaps with the major period of axonal remodeling in the LGN (P1–P21); and the synaptically released zinc has been suggested to play a role in the postnatal refinement of the retinogeniculate projection. It remains unknown why this occurs in only the uncrossed pathway.

Thalamocortical subpopulations in the developing rat barrel cortex

In layer 4, about 37% of the presynaptic terminals identified as zinc-positive at P10 were VGluT2-ir, and in layer 1, the percentage was about 47%. The VGluT2-negative boutons are likely to be cortical in origin, consistent with previous investigations about the source of zinc-positive terminations in the developing barrel cortex (Czupryn & Skangiel-Kramska, 1997; Land & Shamalla-Hannah, 2002).

After our injections of sodium selenite, only about half of the neurons in VPM were labeled by zinc selenite and less than half in Po. There is some possibility that all neurons have the transient zinc-positive phenotype, but that this is expressed at slightly different epochs during the P9–P13 interval. Alternately, the phenotype may be specific to a particular subpopulation. Morphological investigations, for example, have reported thalamocortical afferents with two distinct branching patterns: one group has terminations in layers 1, 4 and 6, and another has terminations only in layers 4 and 6 (Oda *et al.*, 2004). Another study, in mouse barrel cortex, has distinguished two classes of thalamocortical terminations on the basis of their having high or low

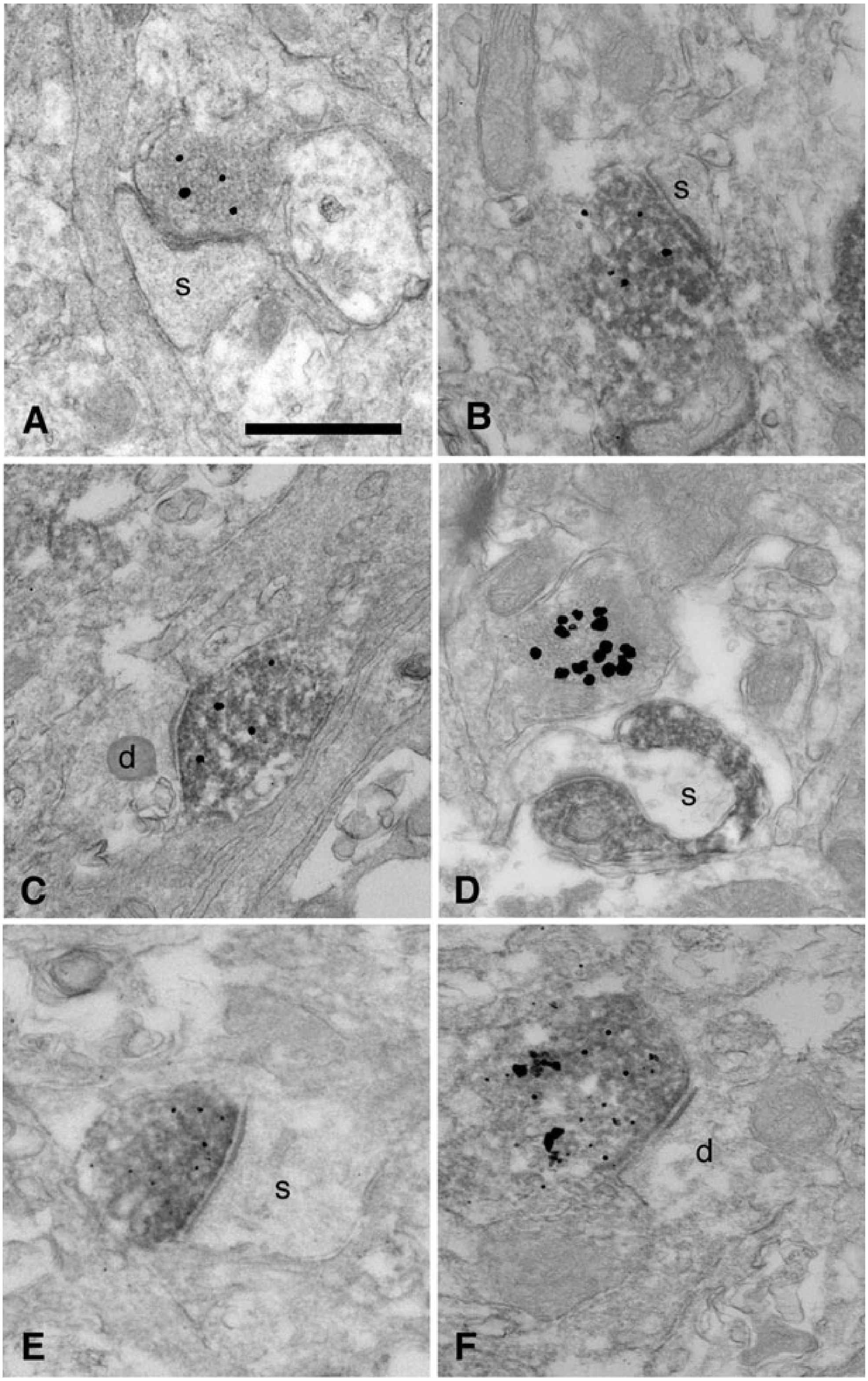

FIG. 4. EMs of zinc-positive terminals and VGluT2-ir terminals in the barrel hollow of P10 pup (A–C) and adult (D), and in layer 1 of P10 pup (E, F). (A) Zinc-positive terminal in a section single-stained for zinc. (B and C) Terminals double-labeled for zinc (silver) and VGluT2 (diaminobenzidine). Synapses are evident on a spine (s) and dendrite (d). (D) In the adult, terminals labeled by zinc can be found in the barrel hollows, but no longer co-localize with VGluT2. (E and F) Terminals in layer 1 double-labeled for zinc (silver) and VGluT2 (diaminobenzidine). Synapses are evident on a spine (s) and dendrite (d). Scale bar, 1 μm.

release probabilities during the period of P4–P22 (Yanagisawa *et al*., 2004). Particularly relevant are immunofluorescence data from developing barrel cortex, which demonstrate that at P7, but not beyond P22, VGluT2-ir terminals are frequently co-localized with VGluT1, a marker for cortico-cortical terminations (Nakamura *et al*., 2005).

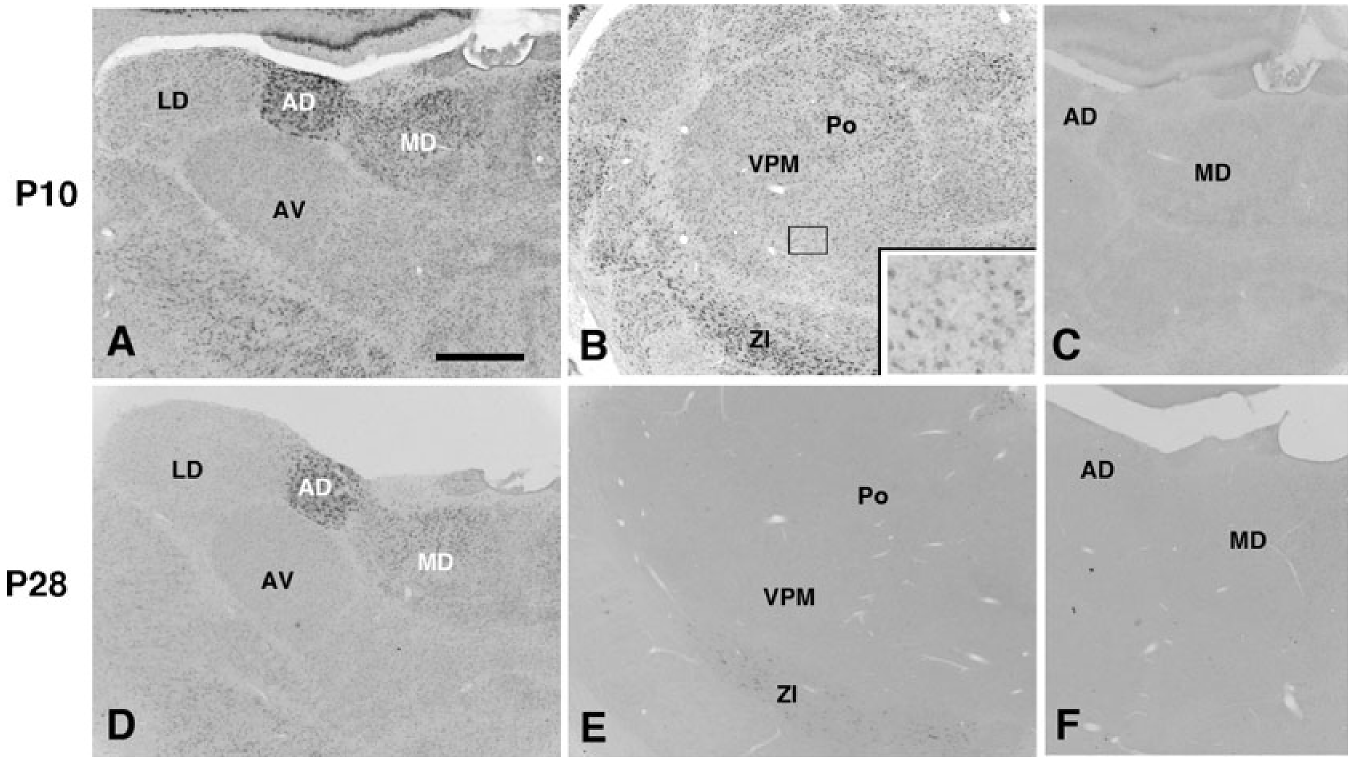

FIG. 5. Micrographs of coronal sections of thalamus at two developmental stages (P10, A and B; P28, D and E) processed for ZnT3 mRNA by *in situ* hybridization. (C and F) Controls, reacted with sense strand-labeled riboprobes. (A, C, D and F) At the level of anterodorsal nucleus (AD), anteroventral nucleus (AV) and mediodorsal nucleus (MD). (B and E) At the level of ventroposterior medial nucleus (VPM) and posterior nucleus (Po). Inset in (B) is the enlarged image from VPM (from rectangle). See text for further description. Scale bar, 500 μm; except for insert in B (100 μm). LD, laterodorsal nucleus.

Thalamocortical terminations transiently take up serotonin (5-HT) from P2.5–P13 in rat barrel cortex (Lebrand *et al*., 1996; Mansour-Robaey *et al*., 1998). While not synthesizing 5-HT, thalamocortical neurons transiently express the genes encoding the serotonin transporter and the vesicular monoamine transporter, suggesting that the 5-HT is stored in vesicles. This period partially overlaps with the time when thalamocortical terminations are zinc-positive in the barrel cortex; and the transient 5-HT phenotype may thus be seen as another indication of stage-specific specializations of the thalamocortical synapses during early postnatal development.

Possible significance of transient zinc-positive synapses for glutamatergic transmission

In the adult cortex, zinc is considered to act as an activity-dependent neuromodulator (see for review, Frederickson *et al*., 2005). Within the glutamatergic system, it potentiates receptors for AMPA (Lin *et al*., 2001), and has a bi-phasic effect for *N*-methyl-D-aspartate (NMDA) (inhibition followed by augmentation; Manzerra *et al*., 2001; Kim *et al*., 2002). What specific action zinc might have on these receptor populations during development is unknown. It may be significant, however, that there is a close temporal coincidence between the transiently zinc-positive terminations and changes that accompany the refinement of thalamocortical circuitry. For example, there is a progressive increase in NR2A subunits, especially at P7 and P12 in barrel cortex (Liu *et al*., 2004). NR2A subunits, according to zinc binding studies in *Xenopus* oocytes, have higher affinity to zinc than does NR2B (Rachline *et al*., 2005). The NR2A subunit has faster deactivation times, which would be expected to result in less calcium entry into cells during activity (Moody & Bosma, 2005). The transient occurrence of zinc-positive synapses might be needed in the transition from slow to faster kinetics in the postsynaptic targets.

The glutamatergic system is closely implicated in neurite outgrowth, of axons (e.g. Tashiro *et al*., 2003; Uesaka *et al*., 2005) or dendrites (e.g. Konur & Ghosh, 2005; Lee *et al*., 2005). In the barrel cortex, thalamocortical axons are still elongating at least until P12 (in layer 4, Agmon *et al*., 1993; in layer 1, Portera-Cailliau *et al*., 2005). The ectopic uptake of 5-HT has been explained as a neurotrophic action on the thalamocortical axons acting through the presynaptic 5-HT1B receptor (Laurent *et al*., 2002; Gaspar *et al*., 2003), and it is possible that synaptic zinc has a similar neurotrophic role, mediated by the glutamatergic transmission system.

The second postnatal week marks the commencement of normal whisking and exploratory behavior (Welker, 1964). It is a period of heightened synaptogenesis and multiple interacting changes in synaptic efficacy and connectional maturation (Micheva & Beaulieu, 1996; De Felipe *et al*., 1997; Patra *et al*., 2004). During development (at least through P14), sensory deprivation by whisker-plucking results in persistent upregulation of zinc in the barrel hollow (Land & Shamalla-Hannah, 2002; see also Czupryn & Skangiel-Kramska, 2003). This seemingly supports some role of zinc in plasticity effects.

While the specific action or actions of transient zinc-positive terminations requires further work, it is interesting to note that the brain-derived neurotrophic factor (BDNF) protein is transiently upregulated in layer 4 of rat somatosensory cortex from P7 to P14 (Das *et al*., 2001). BDNF has pleiotropic roles in many developmental processes, such as regulation of neuronal survival, morphology and neural plasticity (McAllister *et al*., 1997; Itami *et al*., 2003; Hanamura *et al*., 2004; Glebova & Ginty, 2005). These may be in parallel with the influence of synaptic zinc. Alternatively, synaptic zinc may have a direct effect on BDNF. *In vitro* experiments on cultured cortical neurons indicate that zinc is involved in the release of pro-BDNF from cells and its conversion to mature BDNF, by extracellular activation of metalloproteinases (Hwang *et al*., 2005).

Acknowledgements

This work was supported by the Brain Science Institute, RIKEN, by Grant-in-Aid for Scientific Research on Priority Areas – Molecular Brain Science/System study on higher-order brain functions – from the Ministry of Education, Culture, Sports, Science and Technology of Japan, by Grants-in-Aid from the Ministry of Education, Science, Sports and Culture of Japan: Grant number 18500270, and by the Joint Research Program of the National Institute for Basic Biology, Japan. The authors would like to thank Ms Hiroko Katsuno for her expert electron microscopic work and Ms Hiromi Mashiko for her excellent technical assistance. We are grateful to Dr T. Hashikawa and members of his lab for general EM support and advice. These experiments were significantly motivated by discussions with Drs Jeus Perez-Clausell and Neus Miro-Bernie, who proposed the possibility of transient zinc-positive thalamocortical terminations.

Abbreviations

5-HT, serotonin; AD, anterodorsal nucleus; BDNF, brain-derived neurotrophic factor; DIG, digoxigenin; EM, electron microscopy; GRS, granular retrosplenial cortex; ir, immunoreactive; LGN, lateral geniculate nucleus; MGB, medial geniculate body; P, postnatal day; PB, phosphate buffer; PBS, phosphate-buffered saline; PBS-TG, PBS containing 0.5% Triton X-100 and 5% normal goat serum; Po, posterior nucleus; RT-PCR, reverse transcriptase-polymerase chain reaction; SSC, standard sodium citrate; VGluT1, vesicular glutamate transporter 1; VGluT2, vesicular glutamate transporter 2; VPM, ventroposterior medial nucleus; ZnT3, zinc transporter 3.

References

Agmon, A., Yang, L.T., O'Dowd, D.K. & Jones, E.G. (1993) Organized growth of thalamocortical axons from the deep tier of terminations into layer IV of developing mouse barrel cortex. *J. Neurosci.*, **13**, 5365–5382.

Aizenman, E., Stout, A.K., Hartnett, K.A., Dineley, K.E., McLaughlin, B. & Reynolds, I.J. (2000) Induction of neuronal apoptosis by thiol oxidation: putative role of intracellular zinc release. *J. Neurochem.*, **75**, 1878–1888.

Brown, C.E. & Dyck, R.H. (2002) Rapid, experience-dependent changes in levels of synaptic zinc in primary somatosensory cortex of the adult mouse. *J. Neurosci.*, **22**, 2617–2625.

Brown, C.E. & Dyck, R.H. (2004) Distribution of zincergic neurons in the mouse forebrain. *J. Comp. Neurol.*, **479**, 156–167.

Brown, C.E. & Dyck, R.H. (2005) Retrograde tracing of the subset of afferent connections in mouse barrel cortex provided by zincergic neurons. *J. Comp. Neurol.*, **486**, 48–60.

Casanovas-Aguilar, C., Christensen, M.K., Reblet, C., Martinez-Garcia, F., Perez-Clausell, J. & Bueno-Lopez, J.L. (1995) Callosal neurones give rise to zinc-rich boutons in the rat visual cortex. *Neuroreport*, **6**, 497–500.

Casanovas-Aguilar, C., Miro-Bernie, N. & Perez-Clausell, J. (2002) Zinc-rich neurones in the rat visual cortex give rise to two laminar segregated systems of connections. *Neuroscience*, **110**, 445–458.

Casanovas-Aguilar, C., Reblet, C., Perez-Clausell, J. & Bueno-Lopez, J.L. (1998) Zinc-rich afferents to the rat neocortex: projections to the visual cortex traced with intracerebral selenite injections. *J. Chem. Neuroanat.*, **15**, 97–109.

Christensen, M.K., Frederickson, C.J. & Danscher, G. (1992) Retrograde tracing of zinc-containing neurons by selenide ions: a survey of seven selenium compounds. *J. Histochem. Cytochem.*, **40**, 575–579.

Colvin, R.A., Fontaine, C.P., Laskowski, M. & Thomas, D. (2003) Zn2+ transporters and Zn2+ homeostasis in neurons. *Eur. J. Pharmacol.*, **479**, 171–185.

Czupryn, A. & Skangiel-Kramska, Y. (1997) Distribution of synaptic zinc in the developing mouse somatosensory cortex. *J. Comp. Neurol.*, **386**, 652–660.

Czupryn, A. & Skangiel-Kramska, J. (2003) Switch time-point for rapid experience-dependent changes in zinc-containing circuits in the mouse barrel cortex. *Brain Res. Bull.*, **61**, 385–391.

Danscher, G. (1981) Histochemical demonstration of heavy metals. A revised version of the sulphide silver method suitable for both light and electron-microscopy. *Histochemistry*, **71**, 1–16.

Danscher, G. (1982) Exogenous selenium in the brain. A histochemical technique for light and electron microscopical localization of catalytic selenium bonds. *Histochemistry*, **76**, 281–293.

Danscher, G., Norgaard, J.O. & Baatrup, E. (1987) Autometallography: tissue metals demonstrated by a silver enhancement kit. *Histochemistry*, **86**, 465–469.

Das, K.P., Chao, S.L., White, L.D., Haines, W.T., Harry, G.J., Tilson, H.A. & Barone, S. Jr (2001) Differential patterns of nerve growth factor, brain-derived neurotrophic factor and neurotrophin-3 mRNA and protein levels in developing regions of rat brain. *Neuroscience*, **103**, 739–761.

De Biasi, S. & Bendotti, C. (1988) A simplified procedure for the physical development of the sulphide silver method to reveal synaptic zinc in combination with immunocytochemistry at light and electron microscopy. *J. Neurosci. Meth.*, **79**, 87–96.

De Felipe, J., Marco, P., Fairen, A. & Jones, E.G. (1997) Inhibitory synaptogenesis in mouse somatosensory cortex. *Cereb. Cortex*, **7**, 619–634.

Diamond, M.E., Armstrong-James, M. & Ebner, F.F. (1992) Somatic sensory responses in the rostral sector of the posterior group (POm) and in the ventral posterior medial nucleus (VPM) of the rat thalamus. *J. Comp. Neurol.*, **318**, 462–476.

Dyck, R.H., Chaudhuri, A. & Cynader, M.S. (2003) Experience-dependent regulation of the zincergic innervation of visual cortex in adult monkeys. *Cereb. Cortex*, **13**, 1094–1109.

Fabri, M. & Burton, H. (1991) Topography of connections between primary somatosensory cortex and posterior complex in rat: a multiple fluorescent tracer study. *Brain Res.*, **538**, 351–357.

Fox, K. (2002) Anatomical pathways and molecular mechanisms for plasticity in the barrel cortex. *Neuroscience*, **111**, 799–814.

Frederickson, C.J., Koh, J.Y. & Bush, A.I. (2005) The neurobiology of zinc in health and disease. *Nat. Rev. Neurosci.*, **6**, 449–462.

Frederickson, C.J., Rampy, B.A., Reamy-Rampy, S. & Howell, G.A. (1992) Distribution of histochemically reactive zinc in the forebrain of the rat. *J. Chem. Neuroanat.*, **5**, 521–530.

Frederickson, C.J., Suh, S.W., Silva, D., Frederickson, C.J. & Thompson, R.B. (2000) Importance of zinc in the central nervous system: the zinc-containing neuron. *J. Nutr.*, **130** (**5S** (Suppl.), 1471S–1483S.

Fujiyama, F., Furuta, T. & Kaneko, T. (2001) Immunocytochemical localization of candidates for vesicular glutamate transporters in the rat cerebral cortex. *J. Comp. Neurol.*, **435**, 379–387.

Garrett, B., Sorensen, J.C. & Slomianka, L. (1992) Fluoro-Gold tracing of zinc-containing afferent connections in the mouse visual cortices. *Anat. Embryol.*, **185**, 451–459.

Gaspar, P., Cases, O. & Maroteaux, L. (2003) The developmental role of serotonin: news from mouse molecular genetics. *Nat. Rev. Neurosci.*, **4**, 1002–1012.

Glebova, N.O. & Ginty, D.D. (2005) Growth and survival signals controlling sympathetic nervous system development. *Annu. Rev. Neurosci.*, **28**, 191–222.

Hanamura, K., Harada, A., Katoh-Semba, R., Murakami, F. & Yamamoto, N. (2004) BDNF and NT-3 promote thalamocortical axon growth with distinct substrate and temporal dependency. *Eur. J. Neurosci.*, **19**, 1485–1493.

Herkenham, M. (1980) Laminar organization of thalamic projections to the rat neocortex. *Science*, **207**, 532–535.

Hwang, J.J., Park, M.H., Choi, S.Y. & Koh, J.Y. (2005) Activation of the Trk signaling pathway by extracellular zinc. Role of metalloproteinases. *J. Biol. Chem.*, **280**, 11995–12001.

Ichinohe, N., Potapov, D. & Rockland, K.S. (2006) Transient layer-specific zinc-positive phenotype in the developing rat somatosensory cortical system. *FENS Abstr.*, vol. 3, A003.14.

Itami, C., Kimura, F., Kohno, T., Matsuoka, M., Ichikawa, M., Tsumoto, T. & Nakamura, S. (2003) Brain-derived neurotrophic factor-dependent unmasking of 'silent' synapses in the developing mouse barrel cortex. *Proc. Natl. Acad. Sci. USA*, **100**, 13069–13074.

Killackey, H.P. (1983) The somatosensory cortex of the rodent. *Trends Neurosci.*, **6**, 425–429.

Kim, T.Y., Hwang, J.J., Yun, S.H., Jung, M.W. & Koh, J.Y. (2002) Augmentation by zinc of NMDA receptor-mediated synaptic responses in CA1 of rat hippocampal slices: mediation by Src family tyrosine kinases. *Synapse*, **46**, 49–56.

Konur, S. & Ghosh, A. (2005) Calcium signaling and the control of dendritic development. *Neuron*, **46**, 401–405.

Land, P.W. & Aizenman, E. (2005) Zinc accumulation after target loss: an early event in retrograde degeneration of thalamic neurons. *Eur. J. Neurosci.*, **21**, 647–657.

Land, P.W., Buffer, S.A. Jr & Yaskosky, J.D. (1995) Barreloids in adult rat thalamus: three-dimensional architecture and relationship to somatosensory cortical barrels. *J. Comp. Neurol.*, **355**, 573–588.

Land, P.W. & Shamalla-Hannah, L. (2001) Transient expression of synaptic zinc during development of uncrossed retinogeniculate projections. *J. Comp. Neurol.*, **433**, 515–525.

Land, P.W. & Shamalla-Hannah, L. (2002) Experience-dependent plasticity of zinc-containing cortical circuits during a critical period of postnatal development. *J. Comp. Neurol.*, **447**, 43–56.

Land, P.W. & Simons, D.J. (1985) Cytochrome oxidase staining in the rat SmI barrel cortex. *J. Comp. Neurol.*, **238**, 225–235.

Laurent, A., Goaillard, J.M., Cases, O., Lebrand, C., Gaspar, P. & Ropert, N. (2002) Activity-dependent presynaptic effect of serotonin 1B receptors on the somatosensory thalamocortical transmission in neonatal mice. *J. Neurosci.*, **22**, 886–900.

Lebrand, C., Cases, O., Adelbrecht, C., Doye, A., Alvarez, C., El Mestikawy, S., Seif, I. & Gaspar, P. (1996) Transient uptake and storage of serotonin in developing thalamic neurons. *Neuron*, **17**, 823–835.

Lee, L.J., Lo, F.S. & Erzurumlu, R.S. (2005) NMDA receptor-dependent regulation of axonal and dendritic branching. *J. Neurosci.*, **25**, 2304–2311.

Lendvai, B., Stern, E.A., Chen, B. & Svoboda, K. (2000) Experience-dependent plasticity of dendritic spines in the developing rat barrel cortex *in vivo*. *Nature*, **404**, 876–881.

Liguz-Lecznar, M., Nowicka, D., Czupryn, A. & Skangiel-Kramska, J. (2005) Dissociation of synaptic zinc level and zinc transporter 3 expression during postnatal development and after sensory deprivation in the barrel cortex of mice. *Brain Res. Bull.*, **66**, 106–113.

Lin, D.D., Cohen, A.S. & Coulter, D.A. (2001) Zinc-induced augmentation of excitatory synaptic currents and glutamate receptor responses in hippocampal CA3 neurons. *J. Neurophysiol.*, **85**, 1185–1196.

Liu, X.B., Murray, K.D. & Jones, E.G. (2004) Switching of NMDA receptor 2A and 2B subunits at thalamic and cortical synapses during early postnatal development. *J. Neurosci.*, **24**, 8885–8895.

Long, Y. & Frederickson, C.J. (1994) A zinc-containing fiber system of thalamic origin. *Neuroreport*, **5**, 2026–2028.

Lopez-Bendito, G. & Molnar, Z. (2003) Thalamocortical development: how are we going to get there? *Nat. Rev. Neurosci.*, **4**, 276–289.

Lu, S.M. & Lin, R.C. (1993) Related Articles, Links Thalamic afferents of the rat barrel cortex: a light- and electron-microscopic study using Phaseolus vulgaris leucoagglutinin as an anterograde tracer. *Somatosens. Mot. Res.*, **10**, 1–16.

Mansour-Robaey, S., Mechawar, N., Radja, F., Beaulieu, C. & Descarries, L. (1998) Quantified distribution of serotonin transporter and receptors during the postnatal development of the rat barrel field cortex. *Brain Res. Dev. Brain Res.*, **107**, 159–163.

Manzerra, P., Behrens, M.M., Canzoniero, L.M., Wang, X.Q., Heidinger, V. & Ichinose, T., Yu, S.P. & Choi, D.W., (2001) Zinc induces a Src family kinase-mediated up-regulation of NMDA receptor activity and excitotoxicity. *Proc. Natl. Acad. Sci. USA*, **98**, 11055–11061.

McAllister, A.K., Katz, L.C. & Lo, D.C. (1997) Opposing roles for endogenous BDNF and NT-3 in regulating cortical dendritic growth. *Neuron*, **18**, 767–778.

Micheva, K.D. & Beaulieu, C. (1996) Quantitative aspects of synaptogenesis in the rat barrel field cortex with special reference to GABA circuitry. *J. Comp. Neurol.*, **373**, 340–354.

Miro-Bernie, N., Ichinohe, N., Perez-Clausell, J. & Rockland, K.S. (2006) Zinc-rich transient vertical modules in the rat retrosplenial cortex during postnatal development. *Neuroscience*, **138**, 545–557.

Moody, W.J. & Bosma, M.M. (2005) Ion channel development, spontaneous activity, and activity-dependent development in nerve and muscle cells. *Physiol. Rev.*, **85**, 883–941.

Nakamura, K., Hioki, H., Fujiyama, F. & Kaneko, T. (2005) Postnatal changes of vesicular glutamate transporter (VGluT) 1 and VGluT2 immunoreactivities and their colocalization in the mouse forebrain. *J. Comp. Neurol.*, **492**, 263–288.

Oda, S., Kishi, K., Yang, J., Chen, S., Yokofujita, J., Igarashi, H., Tanihata, S. & Kuroda, M. (2004) Thalamocortical projection from the ventral posteromedial nucleus sends its collaterals to layer I of the primary somatosensory cortex in rat. *Neurosci. Lett.*, **367**, 394–398.

Palmiter, R.D., Cole, T.B., Quaife, C.J. & Findley, S.D. (1996) ZnT-3, a putative transporter of zinc into synaptic vesicles. *Proc. Natl. Acad. Sci. USA*, **93**, 14934–14939.

Patra, R.C., Blue, M.E., Johnston, M.V., Bressler, J. & Wilson, M.A. (2004) Activity-dependent expression of Egr1 mRNA in somatosensory cortex of developing rats. *J. Neurosci. Res.*, **78**, 235–244.

Paxinos, G. & Watson, C. (1998) *The Rat Brain in Stereotaxic Coordinates*, 4th Edn. Academic Press, Sydney.

Portera-Cailliau, C., Weimer, R.M., De Paola, V., Caroni, P. & Svoboda, K. (2005) Diverse modes of axon elaboration in the developing neocortex. *PLoS. Biol.*, **3**, e272.

Rachline, J., Perin-Dureau, F., Le Goff, A., Neyton, J. & Paoletti, P. (2005) The micromolar zinc-binding domain on the NMDA receptor subunit NR2B. *J. Neurosci.*, **25**, 308–317.

Riba-Bosch, A. & Perez-Clausell, J. (2004) Response to kainic acid injections: changes in staining for zinc, FOS, cell death and glial response in the rat forebrain. *Neuroscience*, **125**, 803–818.

Schmued, L.C., Albertson, C. & Slikker,W. Jr (1997) Fluoro-Jade: a novel fluorochrome for the sensitive and reliable histochemical localization of neuronal degeneration. *Brain Res.*, **751**, 37–46.

Sugitani, M., Yano, J., Sugai, T. & Ooyama, H. (1990) Somatotopic organization and columnar structure of vibrissae representation in the rat ventrobasal complex. *Exp. Brain Res.*, **81**, 346–352.

Szerdahelyi, P. & Kasa, P. (1986) Histochemical demonstration of copper in normal rat brain and spinal cord. Evidence of localization in glial cells. *Histochemistry*, **85**, 341–347.

Tashiro, A., Dunaevsky, A., Blazeski, R., Mason, C.A. & Yuste, R. (2003) Bidirectional regulation of hippocampal mossy fiber filopodial motility by kainate receptors: a two-step model of synaptogenesis. *Neuron*, **38**, 773–784.

Uesaka, N., Hirai, S., Maruyama, T., Ruthazer, E.S. & Yamamoto, N. (2005) Activity dependence of cortical axon branch formation: a morphological and electrophysiological study using organotypic slice cultures. *J. Neurosci.*, **25**, 1–9.

Valente, T. & Auladell, C. (2002) Developmental expression of ZnT3 in mouse brain: correlation between the vesicular zinc transporter protein and chelatable vesicular zinc (CVZ) cells. Glial and neuronal CVZ cells interact. *Mol. Cell. Neurosci.*, **21**, 189–204.

Waite, P.M. (1973) Somatotopic organization of vibrissal responses in the ventro-basal complex of the rat thalamus. *J. Physiol.*, **228**, 527–540.

Welker, W.I. (1964) Analysis of sniffing of the albino rat. *Behavior*, **22**, 223–244.

Woodroofe, C.C., Masalha, R., Barnes, K.R., Frederickson, C.J. & Lippard, S.J. (2004) Membrane-permeable and -impermeable sensors of the Zinpyr family and their application to imaging of hippocampal zinc in vivo. *Chem. Biol.*, **11**, 1659–1666.

Yanagisawa, T., Tsumoto, T. & Kimura, F. (2004) Transiently higher release probability during critical period at thalamocortical synapses in the mouse barrel cortex: relevance to differential short-term plasticity of AMPA and NMDA EPSCs and possible involvement of silent synapses. *Eur. J. Neurosci.*, **20**, 3006–3018.

Yu, S., Iwatsuki, H., Ichinohe, N., Mori, F. & Shoumura, K. (2001) 'In vivo perfusion Turnbull's reaction' for Fe(II) histochemistry in non-anoxic/non-ischemic and anoxic/ischemic cat brains. *Neurosci. Lett.*, **308**, 79–82.